

This is an Open Access document downloaded from ORCA, Cardiff University's institutional repository: <https://orca.cardiff.ac.uk/id/eprint/125937/>

This is the author's version of a work that was submitted to / accepted for publication.

Citation for final published version:

Sharmin, Tania , Steemers, Koen and Matzarakis, Andreas 2017. Microclimatic modelling in assessing the impact of urban geometry on urban thermal environment. *Sustainable Cities and Society* 34 , pp. 293-308. 10.1016/j.scs.2017.07.006

Publishers page: <http://dx.doi.org/10.1016/j.scs.2017.07.006>

Please note:

Changes made as a result of publishing processes such as copy-editing, formatting and page numbers may not be reflected in this version. For the definitive version of this publication, please refer to the published source. You are advised to consult the publisher's version if you wish to cite this paper.

This version is being made available in accordance with publisher policies. See <http://orca.cf.ac.uk/policies.html> for usage policies. Copyright and moral rights for publications made available in ORCA are retained by the copyright holders.



Microclimatic modelling in assessing the impact of urban geometry on urban thermal environment

Tania Sharmin^{a,1}, Koen Steemers¹, Andreas Matzarakis²

Highlights

- ENVI-met's responsiveness towards measuring Ta and Tmrt is examined.
- Modelling output is compared with field measurements.
- Results show ENVI-met is unable to distinguish among detail urban-geometry features.

Abstract

Diversity in urban geometry can create significant variation in microclimatic conditions. Especially, in tropical warm-humid context, deep urban canyons with variable building heights perform better than uniform canyons, because taller buildings rising above those around them reduce solar gain and enhance wind speed at the pedestrian level. Field measurements in Dhaka comparing the varying traditional urban forms with the more regular formal residential areas have revealed an average air temperature (Ta) difference of 3.3⁰C and a maximum difference of 6.2⁰C, and a mean radiant temperature (Tmrt) difference of 10.0⁰C. The aim of this paper is to understand the responsiveness of the microclimate simulation tool ENVI-met V4 in identifying the variation in urban geometry as reported in the field measurements. The study aims to make specific comparisons between the measured and the simulated data by analysing a particular challenge in complex geometry. It attempts to demonstrate how ENVI-met could benefit from using the correct input as the boundary condition. While the modelling tool aims to produce good results by using synoptic weather information as boundary conditions, this study suggests that it is important to use representative data from the actual site and that hourly input of climatic variables as boundary information can produce the best results. Results show that modelling is able to predict the relative variations in Tmrt conditions between sites, although highly overestimated. However, in terms of Ta, modelling was unable to produce any variations between different urban geometry characteristics. This indicates that, although ENVI-met can produce sufficiently good results in predicting Ta when hourly forcing is used, it is unable to distinguish between the precise details in urban geometry features that can cause significant variations in microclimatic conditions in real situations. Therefore, further assessment of microclimatic variables is needed for using such modelling techniques in order to evaluate the impact of diversity in urban geometry.

Keywords: *ENVI-met V4; urban geometry; morphological diversity; microclimate monitoring; tropical climate*

¹ The Martin Centre for Architectural and Urban Studies, Department of Architecture, University of Cambridge, 1-5 Scroope Terrace, CB2 1PX, Cambridge, United Kingdom.

^aCorresponding author: ts531@cam.ac.uk

² Leiter Medizin-Meteorologie (Head Human-Biometeorology), Deutscher Wetterdienst (German Weather Service)

1.1. Introduction

Urban microclimate is a complex consequence of different parameters which involves innumerable natural and urban processes. The natural parameters like air temperature and humidity, vapour pressure, wind speed, solar radiation, soil temperature and humidity are very sensitive to any 3-dimensional changes in the urban settings. Due to the diverse processes involved, causing different microclimates, one of the most feasible ways to predict their impacts is through the use of numerical methods (Bruse 1999; Arnfield 2003). Numerical modelling and computer simulation techniques are therefore playing increasingly important roles in present day thermal comfort and building performance studies in the urban context. Furthermore, the constraints associated with the in-situ measurements make numerical modelling more convenient for the researchers, especially in terms of comparing theoretical models with different combinations of parameters.

The integration of microclimatic simulation in this study enables the limitations of direct monitoring to be overcome. Direct monitoring and field measurements only allow observation of a few points at a time. It is difficult to measure climatic parameters in a large number of canyons at the same time as it will require multiple sets of equipment and measurement tools which are expensive and involve the risk of theft. Therefore, along with field measurements, ENVI-met V4 (Bruse 2015), a numerical microclimatic tool with high temporal and spatial resolution was used in this study as an important tool for measuring microclimatic dynamics.

The primary interest of using numerical modelling in this study lies in checking its responsiveness in identifying the diversity in urban forms. Studies in the mid-latitude and tropical climate cities have shown that even though deep urban canyons can improve daytime microclimate, they could generate a nocturnal urban heat-island effect (Qaid & Ossen 2014). Due to the inconsistency between day and night situations, uniform, homogeneous canyons are not climatically ideal for a tropical, hot-humid climate. A field measurement by Sharmin et al. (2015) in the tropical megacity Dhaka reveal, varying traditional urban forms are cooler in comparison to more regular formal residential areas.

Therefore, the study examines the proficiency of a numerical modelling tool ENVI-met V4 in distinguishing uniform versus variable urban geometry conditions as identified during the field measurements. It aims to quantify the microclimatic differences measured between the actual case-study areas with variable and uniform geometry, mainly in terms of air temperature and mean radiant temperature and, subsequently, to compare the differences with the modelled variations. The objective is full-filled in a series of analysis: firstly, by examining ENVI-met's ability in reproducing microclimatic conditions as observed in field-study conditions with the use of site-specific measured data as input for simulation models. Secondly, by examining ENVI-met's responsiveness to the diversity in urban geometry by using the same input data for each case-study site. In this case, it is assumed that whatever difference is occurring between the microclimate of different sites, is due to the variation in their urban geometry. It attempts to answer the research questions:

- To what extent ENVI-met modelling can reproduce the microclimatic conditions for the existing case-study areas by using field measurements as boundary conditions?
- Is ENVI-met able to recognise the diversity in urban form when all case-study areas are modelled using identical boundary condition?

ENVI-met is an advanced simulation system that recreates the microclimatic dynamics of the outdoor environment by addressing the interaction between climatic parameters, vegetation, surfaces, soil and the built environment (Bruse & Fleer 1998). The new features in ENVI-met V4 include the simple forcing of air temperature and humidity in 2m levels which needs input data, such as the initial temperature of the atmosphere, specific humidity at the model top and maximum and minimum values over a 24h cycle. The forcing also has the option to input the values on an hourly basis which are collected either from weather stations or directly from on-site measurements. This study uses simple forcing together with the hourly forcing (for air temperature and humidity) options to perform simulation of the case-study areas.

ENVI-met has been extensively used in urban design and thermal comfort studies for its ability to reproduce microclimatic conditions within the urban canopy layer (UCL) (Ali-Toudert & Mayer 2007; Krüger et al. 2011a; Ng et al. 2012). Although there are several microclimatic tools such as RayMan (Matzarakis et al. 2010), SOLWEIG (Lindberg et al. 2008) and Townscope (Teller & Azar 2001), ENVI-met is particularly popular for its high temporal and spatial resolution, its advanced 3D interface and modelling techniques and its

ability to adjust air temperature and relative humidity. The latest version (ENVI-met V4) considers the heat capacity of the building materials (Huttner 2012; Yang et al. 2013), a unique feature that other microclimatic simulation tools are yet to accomplish. ENVI-met is based on the fundamental laws of fluid dynamics and thermodynamics, while other models such as RayMan and SOLWEIG are 3D radiation models. It is thus a rare example of a model which can be used to explore the relationships between urban form and the urban microclimate.

The study has been carried out in three steps, named as Step 1 to Step 3. Firstly, in Step 1, field measurements of microclimatic dynamics are discussed. Secondly, actual case-study areas are modelled in ENVI-met V4 (Step 2) and a comparison of microclimatic conditions between the modelled sites is carried out. Actual microclimatic measurements from the field-study are used as the model boundary conditions. Thirdly, in Step 3, the same case-study areas are modelled using boundary conditions from the worst-case scenario, obtained from the EPW (EnergyPlus Weather) data for Dhaka. In this step, all sites have the same boundary conditions in order to understand how they respond to the differences in urban form. Finally, microclimatic deviations among the case-study areas reported from modelling in the second and third steps are evaluated against the actual differences reported in the field measurements. The results particularly identify the limitations of the microclimatic simulations in terms of predicting air temperature and mean radiant temperature.

1.2. Uniform versus variable urban geometry

The geometry of urban canyons has been proven to play a key role in determining the heat island effect and affecting thermal comfort in streets. By definition the urban canyon is a basic geometric unit estimated by a two-dimensional cross-section of buildings (Oke 1988). The urban geometry parameters used in this study are H/W ratio and sky view factor (SVF). H/W ratio is a key urban geometry parameter affecting the incoming and outgoing solar radiation, radiation flux and wind flow in an urban canyon (Xi et al. 2012). Here, H is the average height of the canyon walls and W is the canyon width (Oke 1988). Sky view factor (SVF) on the other hand, is defined as the ratio of the amount of sky visible from a given point on the ground to the potentially available sky hemisphere subtended by a horizontal surface (Oke 1987). SVF, which is dimensionless and ranges from 0 to 1, is an important parameter to measure urban heat island (UHI) impact (Kikegawa et al. 2006). Studies such as (Bourbia & Awbi 2004; Tan et al. 2014; Yan et al. 2014) have shown that lower SVF is associated with

lower daytime air temperature by creating a cool island effect. While the wider study uses other parameters to describe the geometry or physical form of urban canyons, such as street orientation, surface-to-volume ratio and form factor, the main discussion in this paper focuses on H/W ratio and SVF.

Inside the urban canyon, the flanking buildings are assumed to be repetitive and semi-infinite in length. Several studies have confirmed that deep urban canyons can aid in reducing air temperature during day-time in comparison to wider canyons (Shashua-Bar et al. 2004; Khandaker Shabbir Ahmed 1994; Emmanuel & Johansson 2006; Bourbia & Boucheriba 2010; Johansson 2006; Colaninno et al. 2011). This implies that urban planners should be encouraged to propose deeper urban canyons in places where protection from solar gain could provide better thermal comfort and lower surface temperatures. However, a potential conflict arises at night times when deep canyons tend to trap long-wave radiation released in the urban canyons and subsequently, creates a nocturnal UHI impact (Arnfield 2003; Oke et al. 1991). An important phenomenon is overlooked in this discussion as it assumes urban canyons as having a uniform character with uniform building heights and plot sizes. This is an acceptable simplification when assessing the larger urban boundary layer³ but not with respect to the more local conditions within the urban canopy layer⁴. Street canyons are typically defined by height-to-width (H/W) ratio, as mentioned above, that is assumed to remain constant throughout the length of the canyon. This can be appropriate for many planned modern urban settlements specially those emerging from concepts where “zoning in urban planning produces homogeneous contiguous blocks”(Colaninno et al. 2011).

In contrast to this notion of homogeneity, recent research has called for more investigation of urban diversity: “Surface heterogeneity dominates from neighbourhood to regional scales and should be more strongly considered in future studies” (Barlow 2014). Likewise, Ratti (2005) and Chen et al. (2012) has pointed out that real cities often represent irregular building patterns in urban canyons. Studies have shown that diversity may further improve our understanding of the urban microclimate (Steemers & Ramos 2010). Thus, examining city’s microclimate ignoring its physical diversity can produce improper outcomes.

³ Urban boundary layer (UBL) is the lowest part of the atmosphere, is defined as the entire volume of air above the city that is influenced by its surface characteristics and by the activities within it (Erell et al. 2012).

⁴ Urban Canopy Layer (UCL) is defined as the space between the buildings extending up to the roof level of the buildings at which climatic variables such as air temperature, humidity, vapour pressure, wind speed, solar radiation and soil temperature and humidity are sensitive to any 3-dimensional changes in the urban settings (Erell et al. 2012).

Not only that; incorporating diversity could be a key solution to prevent the contradictory role of deep urban canyons between day and night.

‘Diversity in urban geometry’ refers to the concept of ‘randomness’ as coined by Steemers et al. (1997) in their seminal work on city texture and microclimate and can be defined as the variation in building height, grid size and street width. Although the variation in grid sizes was not explored in this study, the variation in building height and street width is taken into consideration by using the H/W ratio. Diversity or the complexity of urban geometry has been identified by the standard deviation of H/W ratio.

This study is an extension of the preceding research by Sharmin et al. (2015) that showed that urban canyons with variable aspect ratios and diversity in urban form could reduce air temperature by 1.0⁰C - 4.0⁰C in comparison to uniform urban canyons. In the study, traditional residential areas⁵ with diverse building heights and aspect ratios were compared with formal residential areas⁶ with regular urban characteristics. The comparison between the two revealed that traditional residential areas performed better in terms of microclimate as well as pedestrian thermal comfort. As a continuation of the above research, this study is carried out using microclimatic model ENVI-met V4 (Bruse 2015) to review the model’s ability to differentiate between variable versus uniform urban geometry conditions.

1.3. Methodology

1.3.1. Introduction to microclimatic simulation tool: ENVI-met

ENVI-met is a CFD microclimatic model to simulate the interactions between building, pavement and natural surfaces in a virtual environment by reproducing the major atmospheric processes (Bruse 1999). This involves a sequence of mathematical calculations established by the laws of fluid dynamics and thermodynamics which govern the atmospheric motions. It is a non-hydrostatic, RANS⁷ model with a typical horizontal resolution from 0.5 to 10 m, a time frame of 24-48 hours and a time-step of 1-5 seconds. This high resolution is particularly helpful

⁵ LCZ classification is compact mid-rise as per (Stewart & Oke 2012). Stewart and Oke (Stewart & Oke 2012) suggested a new system of climate-based classification of cities, called “local climate zones” (LCZs), that is: “inclusive of all regions, independent of all cultures, and, for heat island assessment, quantifiable according to class properties that are relevant to surface thermal climate at the local scale”.

⁶ LCZ classification is again compact mid-rise.

⁷ Reynolds-averaged Navier–Stokes equations to calculate turbulent flows

for identifying pedestrian comfort issues and interactions between individual buildings, surfaces, and plants (Ali-Toudert & Mayer 2007; Bruse 1999).

1.3.2. Limitations in ENVI-met

ENVI-met has certain limitations.

Air flow

Wind speed and its direction remain constant throughout the simulation period although it is modified by the built structures and vegetation once it enters the model domain. Also, model accuracy is reduced if the input wind speed is greater than 2m/s (Krüger et al. 2011).

Turbulence

ENVI-met uses the standard $k - \varepsilon$ closure model for calculating turbulence. A problem with this model is that it tends to overestimate the turbulence production (k) in areas with high acceleration or deceleration, especially when air flow is modified by an obstacle. The Kato-Launder modification [Kato and Launder (1993), cited in Huttner (2012)] is able to reduce the problem to some extent, however, the application of this makes the simulation more likely to numerical instabilities. Other solutions to this, such as Direct Numerical Simulations (DNS) or Large Eddy Simulation (LES), require a complete reprogramming of ENVI-met which is deemed to be infeasible in the near future.

Radiation

ENVI-met has some issues with the calculation of radiation fluxes (Huttner 2012).

- The scattering of diffuse radiation towards upward and downward directions is considered isotropic⁸.
- Diffused short wave radiation is not absorbed while passing through plants (Yang et al. 2013).
- When direct short wave radiation passes through plants no diffused short wave radiation is generated.
- Short wave radiation reflected upward from the ground and plants are not counted.
- Long wave radiation emitted by vegetation and other different surfaces is not calculated on the basis of each surface category; rather, it is calculated on the basis of an average temperature of all surfaces within the field of view.

⁸ In Physics, an isotropic object or substance has a physical property of having the same value when measured in different directions. The object is often contrasted with the anisotropic.

Due to the errors in estimating direct short wave and diffused/reflected short wave and long wave radiation, the calculation of T_{mrt} may produce major deviations from on-site measurements.

Air temperature

Air temperature in ENVI-met is calculated by the combined advection-diffusion equation in which the change in air temperature is affected by the deviation of the long wave radiation (Huttner 2012). The equations do not consider the heating and cooling of air layers due to a divergence of vertical long wave radiation. The long wave fluxes inside urban environments are too complex to be included in ENVI-met model as they are driven by both vertical as well as horizontal fluxes. The recent version of ENVI-met V4 has shown improvement in recognising the long wave flux divergence. However, the variation in air temperature due to larger regional effects are excluded. For example, Maggiotto et al. (2014) have discussed the performance of the temperature perturbation-type ADMS-Temperature and Humidity Model (ADMS-TH) and the CFD-based model ENVI-met 3.1 for the prediction of urban air temperature. In their study, using measurements collected in the city of Lecce in Italy in summer 2012, ADMS-TH predicted the temperature cycle with higher accuracy than ENVI-met.

Computation time

As far as mathematical computation is concerned, it is very complicated to carry out a full three-dimensional calculation of microclimatic dynamics of a large urban area (Ratti 2005). Many recent versions of the built environment software, such as AutoCAD (Autodesk, <http://www.autodesk.com>), can easily carry out simple mathematical algorithms like shadow casting. These do not impose any problem for an individual or a small number of buildings, but as soon as they reach an urban scale, the computation collapses due to excessive vectorial complexity. From this perspective, since ENVI-met is adopting a holistic approach to compute fine details at an urban scale, it is not surprising that the computation time and computer power are substantial. This makes the model less user-friendly. Despite the fact that ENVI-met has one of the highest spatial resolutions available for microclimatic modelling, a compromise has to be made to reduce the computation time. As a consequence, even with fairly high resolutions like 2m x 2m, many detailed morphological aspects are disregarded which has significant consequences on solar exposure and thus affecting the radiation budget.

Despite such limitations, ENVI-met is a reputable model that is widely validated and used for urban microclimate assessment, and the only one that has features and capabilities necessary for the study in hand.

1.3.3. Study area

The study was carried out in six urban canyons in four different residential areas in Dhaka with different urban geometry characteristics. The residential areas can be categorised into two types: traditional and formal. The traditional residential areas (TRA) are characterised by a compact built environment, high density, high aspect ratio, winding street pattern and variable building height. On the other hand, formal residential areas (FRA) also have a compact built form and a high-density settlement; but a lower aspect ratio with streets arranged in a grid-iron pattern and most importantly, a uniform building height. The traditional residential areas in this study are called *South Kafrul* and *Mid-Kafrul* and the formal residential areas are called *Mahakhali DOHS* and *Baridhara DOHS*. Table 1 includes a list of abbreviated site names for the case-study areas as well as their urban geometry information.

Table 1. Abbreviated site names and urban geometry characters

| Microclimate site name | Actual name | Abbreviated name | sky view factor | canyon aspect ratio | building height range (m) or, mean |
|--------------------------------|-----------------------|------------------|-----------------|---------------------|------------------------------------|
| Traditional Area 1 East-West | <i>South Kafrul</i> | TRA1EW | 0.113 – 0.331 | 1 – 4 | 10 – 29 |
| Traditional Area 1 North-South | <i>South Kafrul</i> | TRA1NS | | | |
| Traditional Area 2 North-South | <i>Mid Kafrul</i> | TRA2NS | 0.133 – 0.168 | 1.8 - 3.5 | 10 - 16 |
| Formal Area 1 East-West | <i>Mahakhali DOHS</i> | FRA1EW | 0.169 – 0.277 | 2 – 2.5 | 20 |
| Formal Area 2 East-West | <i>Baridhara DOHS</i> | FRA2EW | 0.229 – 0.259 | 1.2 – 1.8 | 20 |
| Formal Area 2 North-South | <i>Baridhara DOHS</i> | FRA2NS | | | |

The building heights in the traditional areas are ranged from 10-29m with a 70-80% ratio of the built-up area. An east-west and a north-south oriented urban canyon are selected in the traditional area *South Kafrul* (TRA1), namely, TRA1EW and TRA1NS. These are mixed-use residential neighbourhoods with a combination of diverse building heights and building separations, mostly paved land cover, and narrow streets. In the second traditional site, *Mid Kafrul* (TRA2), only one urban canyon (north-south oriented) is considered suitable for conducting the survey. The canyon is termed as TRA2NS. The height variability is lesser than the former site and the streets are narrower.

The formal residential areas are on the other hand planned residential areas with mostly uniform building heights (generally 6 storey apartment buildings) with wider street widths compared to the traditional areas. The case-study areas include an east-west oriented urban canyon in the formal residential area *Mahakhali DOHS* (FRA1) and another east-west and a north-south oriented urban canyon in *Baridhara DOHS* (FRA2). The canyons are termed as FRA1EW, FRA2EW and FRA2NS respectively. The areas have an average building height of 20m with a 60-70% built up area ratio.

1.3.4. Microclimatic monitoring

Meteorological monitoring was conducted for four days in September 2014 (Autumn 2014) and four days in May and June in 2015 (Summer 2015). The initial idea was to monitor the same sites over the two years. However, the monitoring in site TRA1NS in 2015 was discarded due to logistic problems. Field measurements included air temperature, relative humidity, wind speed and globe temperature. Globe temperature was subsequently used to calculate mean radiant temperature (T_{mrt}). The study did not intend to investigate nocturnal urban heat island conditions. Therefore, measurements were taken between 9:00-18:00 and at 1.1m height and at least 1m distant from the nearby buildings in the street. The specific height of 1.1m represents the gravitational centre for an average height human body (ISO 7726 1998). The measurement point was typically chosen around the middle of the length of the canyon so that the measurements are representative of the microclimatic conditions of the respective canyon. Thus, the effect of the neighbouring streets, and particularly street junctions, is slightly reduced. Figure 1 shows the measurement points at the traditional and formal sites.

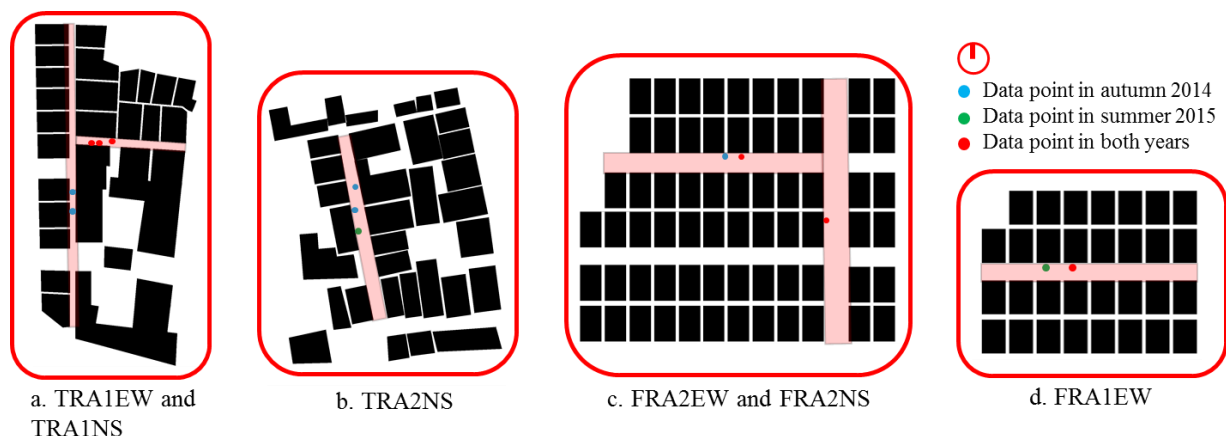


Figure 1. Measurement points at the traditional and formal sites: a. TRA1EW and TRA1NS, b. TRA2NS, c. FRA2EW and FRA2NS and d. FRA1EW

Error! Reference source not found. lists the name, range and accuracy of the instruments used in the study compared against ISO standards (ISO 7726 1998). Tiny-tag data loggers were used to measure air temperature and humidity. Wind speed was measured with a three-cup anemometer at the same height (1.1 to 1.2m) recorded with an OM-CP-WIND101A data logger⁹. Globe temperature was measured using a Tiny-tag data logger with a thermocouple thermistor probe. It consisted of a 40mm ping-pong ball painted in Humbrol matte grey¹⁰ and the thermistor probe inserted inside the ball. This is a widely accepted approach for measuring globe temperature as verified in previous research (Thorsson et al. 2007; de Dear 1987).

Table 2. Measuring range and accuracy for the instruments used in the study

| Name of the instrument | Range of the instrument | Accuracy of the instrument |
|---|-------------------------|--|
| Tinytag Ultra 2 Temperature/ Relative Humidity Logger | -25 to +85°C | Better than $\pm 0.5^\circ\text{C}$ |
| Tinytag Plus 2 Temperature Logger for Thermistor Probe PB-5001 | -40 to +125°C | Logger: Better than $\pm 0.35^\circ\text{C}$, when used with PB-5001 |
| OM-CP-WIND101A-KIT Series | 0 to 44.704 m/s | ± 2.0 mph from 0 to 10 mph; $\pm 2.5\%$ of reading from >10 to 100 mph |
| Tinytag Ultra 2 Temperature/Relative Humidity Logger | 0 to 95% RH | $\pm 3.0\%$ RH at 25°C |

1.3.5. Step 1: measurements

Step 1 represents the field-study measurements carried out in actual sites. The results section reviews the variation between the formal (FRA2) and traditional (TRA1) residential areas in terms of air temperature and mean radiant temperature. Results are presented in the form of boxplots showing summary of air temperature and mean radiant data during 12:00-15:00 (see Figure 4, Figure 5, Figure 7, Figure 8). Next, the progression of the above parameters during 09:00-17:00 is presented (Figure 6). The reason for choosing the period between 12:00-15:00 for boxplot analysis is that the impact of geometry on microclimate is more clearly visible when it is observed over a certain period of the day, rather than observing the average

⁹ The anemometer employed in this study is more appropriate for meteorological stations and high wind speeds, and not as ideal for low level wind speeds in urban streets, or areas with turbulence (See Table 2). Therefore, low wind speeds in formal residential areas could be slightly underestimated.

¹⁰ The study did not specify the reflectance of the ‘Humbrol matte grey’ colour used for the ping-pong ball for the globe thermometer. Literature suggests that grey colour of 0.3 reflectance should be used for outdoor conditions.

value taken over the total day-time hours. Therefore, 12:00-15:00 is chosen when solar radiation is more dominant and air temperature is generally the highest.

1.3.6. Step 2: ENVI-met V4 model based on measurements

After reviewing the field measurements across the autumn 2014 and summer 2015 data in Step 1, the Step 2 specifically concentrates on to two sites - TRA1 (traditional area 1) and FRA2 (formal area 2) - for further analysis using microclimatic simulations. The study has made this simplification in order to be able to proceed with the analysis. Although microclimatic simulation for all case-study sites would be ideal, this is not necessary for this particular exercise purpose where the main intention is to examine whether or not ENVI-met is able to distinguish between the urban geometry variations occurring between the traditional and the formal areas. Since TRA1 and FRA2 clearly represent the respective morphological characters of the traditional and the formal areas, it is sufficient to compare these two sites for the purpose of this study.

Table 3. Geometry parameters of the case-study models

| TRA1EW | | | TRA1NS | | | FRA2EW | | | FRA2NS | | |
|--------------------|-----------|-------|----------|-----------|-------|----------|-----------|-------|----------|-----------|-------|
| Receptor | H/W ratio | SVF | Receptor | H/W ratio | SVF | Receptor | H/W ratio | SVF | Receptor | H/W ratio | SVF |
| A1 | 3.5 | 0.156 | C1 | 4.5 | 0.108 | B1 | 1.8 | 0.205 | D1 | 1.3 | 0.239 |
| A2 | 3.5 | 0.145 | C2 | 4.5 | 0.116 | B2 | 1.8 | 0.265 | D2 | 1.3 | 0.289 |
| A3 | 2.8 | 0.155 | C3 | 3.5 | 0.098 | B3 | 1.8 | 0.209 | D3 | 1.3 | 0.239 |
| A4 | 2.8 | 0.156 | C4 | 3.5 | 0.113 | B4 | 1.8 | 0.192 | D4 | 1.3 | 0.239 |
| A5 | 3.3 | 0.156 | C5 | 2.6 | 0.143 | B5 | 1.8 | 0.238 | D5 | 1.3 | 0.281 |
| A6 | 3.3 | 0.132 | C6 | 2.6 | 0.204 | B6 | 1.8 | 0.2 | D6 | 1.3 | 0.239 |
| | | | | | | B7 | 1.7 | 0.21 | D7 | 1.3 | 0.236 |
| | | | | | | B8 | 1.7 | 0.284 | D8 | 1.3 | 0.299 |
| | | | | | | B9 | 1.7 | 0.225 | D9 | 1.3 | 0.236 |
| Average | 3.17 | 0.15 | | 3.53 | 0.13 | | 1.77 | 0.23 | | 1.30 | 0.26 |
| Standard deviation | 0.342 | 0.010 | | 0.850 | 0.039 | | 0.050 | 0.031 | | 0.000 | 0.026 |

Step 2 presents the simulation modelling of the actual case-study areas using the field measurement data as the boundary conditions. The urban canyons TRA1EW, TRA1NS, FRA2EW and FRA2NS are modelled (Figure 2, Figure 3). The simulations were carried out for two days in September 2014 similar to the field measurements in autumn 2014. Urban geometry parameters of the case-study models are presented in Table 3. Here, standard deviation of H/W ratio gives an indication of the diversity of urban form in the traditional area TRA1EW and TRA1NS compared to the same in the formal area FRA2EW and FRA2NS.

Simulations were started from 04:00 local time (UTC+6), approximately 2 hours before sunrise. The total modelling time was 20 hours. The initial 4-hour data is excluded from analysis because it is considered as the model ‘spin up’ period. 1D vertical profiles (from the ground surface to 2500 m height) of atmospheric parameters (such as specific humidity) were collected from the University of Wyoming Radiosonde data (<http://weather.uwyo.edu/upperair/sounding.html>). Other microclimatic information such as air temperature, relative humidity and wind speed and direction were collected from field measurements. A detail of input data can be found in Table 4.

Instead of a single point measurement, an average value of multiple measurement points has been used in the simulation models. The measurement points (receptors) are denoted by A1-A6 for TRA1EW, C1-C6 for TRA1NS, B1-B9 for FRA2EW and D1-D9 for FRA2NS as shown in Figure 2(e, f) and Figure 3 (e, f) respectively. This is to acquire a more general information about the microclimatic condition inside the canyon rather than having information of a particular point and thus to avoid any bias imposed by a single measurement point. Since, such model generates approximate results, it was assumed to be more appropriate to compare the average values from simulation models with the actual measurement values. For example, globe temperature and subsequently, Tmrt values may differ across the street canyon depending on the position of the sun and shade. Therefore, it was assumed to be better to use an average value for comparison with actual measurements. However, air temperature, relative humidity and wind speed variations across the same vertical height were found to be negligible inside the canyon. Therefore, it was not essential to use an average value from the simulation model for these parameters.

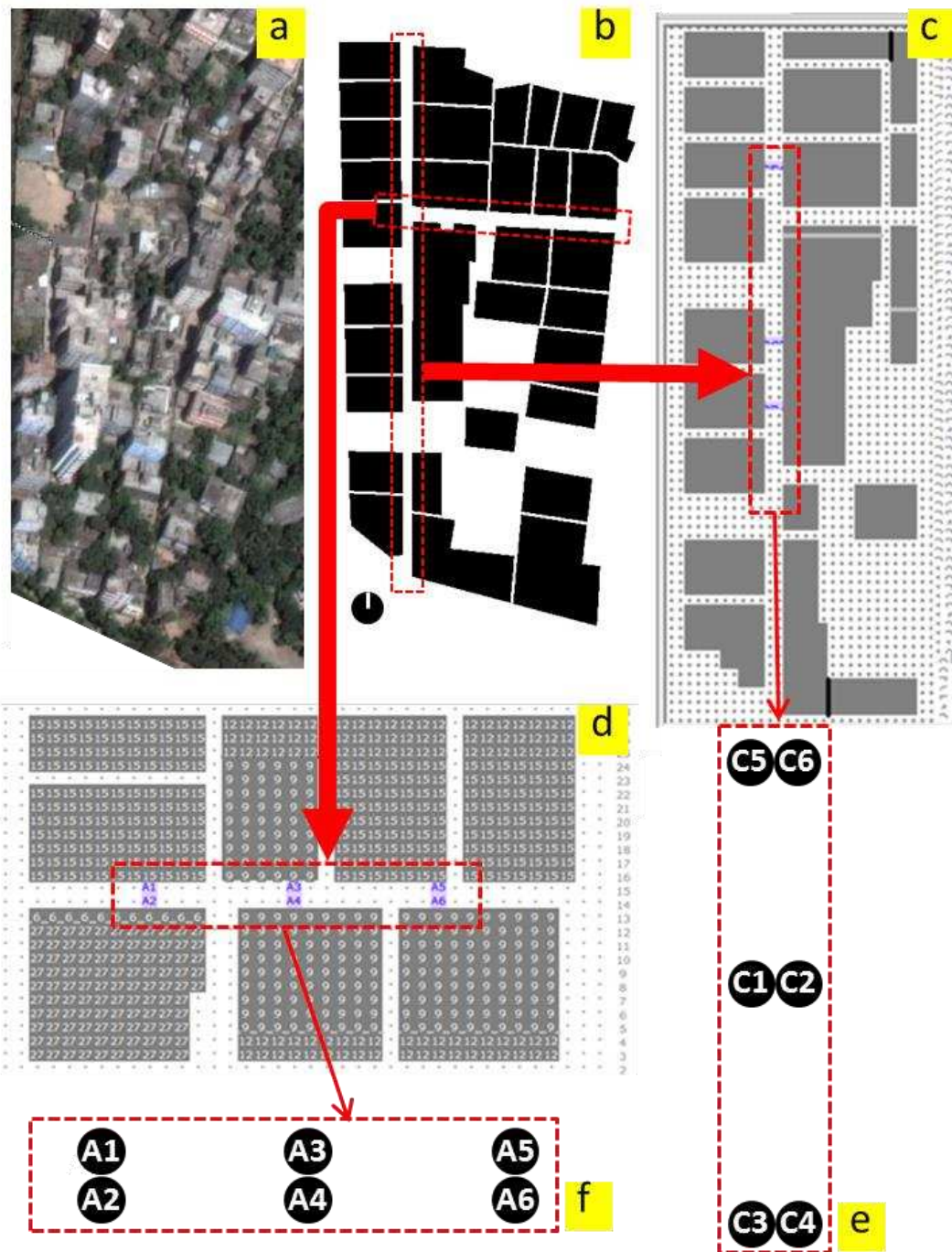


Figure 2. Case-study models for the traditional area TRA1EW and TRA2NS showing: a) Google maps, b) figure-ground drawings, c) ENVI-met model for TRA1NS, d) ENVI-met model for TRA1EW e) receptor points in TRA1NS and f) receptor points in TRA1EW. Map data ©2015 Google Earth, Dhaka, Bangladesh. Source: “Dhaka” 23°46’02.75” N and 90°25’10.32” E. Google Earth. January 07, 2015. April 20, 2015. (Earth 2015)

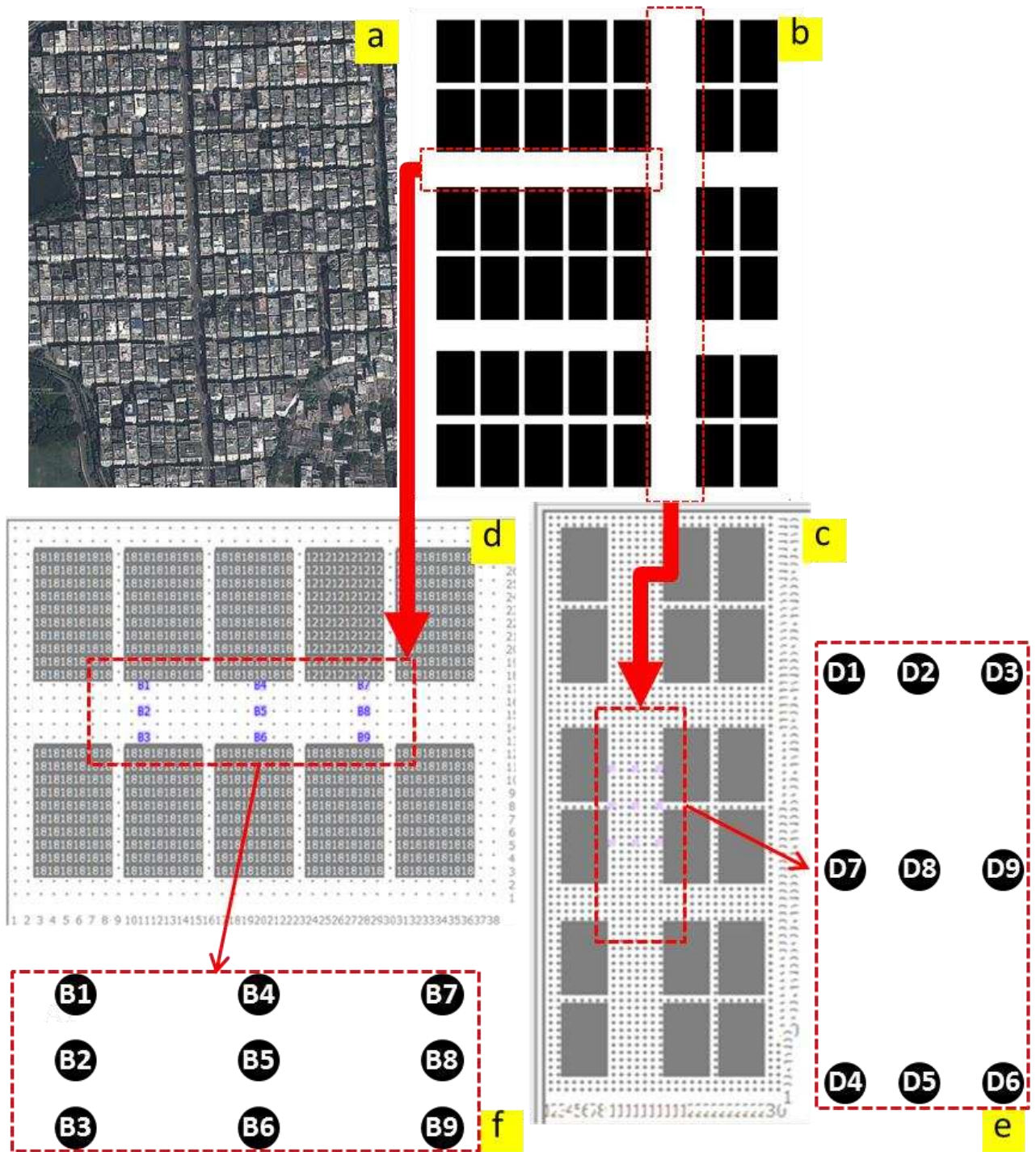


Figure 3. Case-study models for the formal area FRA2EW and FRA2NS showing: a) Google maps, b) figure-ground drawings, c) ENVI-met model for FRA2NS, d) ENVI-met model for FRA2EW e) receptor points in FRA2NS and f) receptor points in FRA2EW. Map data ©2015 Google Earth, Dhaka, Bangladesh. Source: “Dhaka” 23°46’02.75” N and 90°25’10.32” E. Google Earth. January 07, 2015. April 20, 2015. (Earth 2015)

Table 4. Input data for case-study models in Step 2

| | TRA1EW | TRA1NS | FRA2EW | FRA2NS |
|--|---|--|--|---|
| Canyon orientation | east-west (EW) | north-south (NS) | east-west (EW) | north-south (NS) |
| Model area | | | | |
| Main Model Area | 76m x 58m | 60m x 156m | 76m x 58m | 60m x 156m |
| Grid Size in metre | dx=2, | dx=2, | dx=2, | dx=2, |
| Dx = size of X grid | dy=2, | dy=2, | dy=2, | dy=2, |
| Dy = size of Y grid | dz=3 | dz=3 | dz=3 | dz=3 |
| Dz = size of Z grid | | | | |
| Construction material | | | | |
| Building Material | Wall: 10" brick wall (burned), Roof: light-weight concrete | same | same | same |
| Soil | Road: asphalt, Pavement: paved concrete-grey | same | same | same |
| Position | | | | |
| Longitude ($^{\circ}$) | 90.23 | same | same | same |
| Latitude ($^{\circ}$) | 23.24 | same | same | same |
| Start and duration of the model | | | | |
| Date of simulation | 16/09/2014 | 16/09/2014 | 26/09/2014 | 26/09/2014 |
| Start time | 04:00 | same | same | same |
| Total simulation time (h) | 20 | same | same | same |
| Initial meteorological conditions | | | | |
| Roughness length at measurement site | 0.1 | same | same | same |
| Initial temperature of atmosphere ($^{\circ}$ C) | 30.86 $^{\circ}$ C | 30.33 $^{\circ}$ C | 31.63 $^{\circ}$ C | 30.67 $^{\circ}$ C |
| Simple forcing: Air temperature (K) | Min 301 at 05:00; Max 309.5 at 11:00 | Min 300, at 5:00; Max 309.1, at 11:00 | Min 301 at 5:00; Max 311.6 at 12:00 | Min 301 at 5:00; Max 309.3, at 12:00 |
| Simple forcing: Relative humidity (%) | Min 57 at 11:00; Max 87, at 05:00 | Min 58, at 11:00; Max 90, at 05:00 h | Min 51 at 14:00; Max 88, at 05:00 | Min 61 at 12:00; Max 88, at 05:00 |
| Specific humidity at model top (2500 mg/kg) | 9 | 9 | 10.8 | 10.8 |
| Wind speed measured at 10m height (m/s) | 4.5 | 4.5 | 0.5 | 0.5 |
| Wind direction (deg) ($^{\circ}$) = from North, 180 $^{\circ}$ = from South) | 135 | 135 | 135 | 135 |
| Cover of low clouds (octas) | 2 | 2 | 2 | 2 |
| Cover of medium clouds (octas) | 2 | 2 | 2 | 2 |
| Cover of high clouds (octas) | 2 | 2 | 2 | 2 |
| Soil data, for all models | | | | |
| | Soil layer (name) | Soil layer (cm) | Soil Wetness (%) | Initial temperature (K) |
| | Upper layer | 0 – 20 cm | 50 | 293 |
| | Middle layer | 20 – 50 cm | 60 | 293 |
| | Deep layer | 50 – 200 cm | 60 | 293 |
| | Bedrock layer | Below 200 cm | 60 | 293 |

1.3.7. Step 3: ENVI-met model based on worst-case boundary conditions

Step 3 presents the simulation modelling of the actual case-study areas using identical boundary conditions for each model. This means the main difference between Step 2 and Step 3 lies in the boundary conditions. Similar to Step 2, Step 3 also examines the microclimatic variables resulting from the simulation of the four real urban canyons (Figure 2, Figure 3) and then compares the inter-site-variations for the simulation models. The inter-site-variations for the simulation models are then compared with the inter-site-variations recorded during the field measurements.

The intention of this study is to test whether ENVI-met is able to distinguish the geometry variations between sites. One way to test this is to keep the boundary conditions the same across all case-study areas. Therefore, identical climatic information from EPW (EnergyPlus Weather) data for Dhaka was used as the model boundary conditions. A worst-case scenario with high air temperature and high humidity is assumed for the study. The worst-case scenario was determined from the EPW (EnergyPlus Weather) data for Dhaka (<http://apps1.eere.energy.gov/buildings/energyplus>). The climatic information for a hot-humid summer day (April 5, 2014) was selected for the study to represent a worst-case scenario. Wind conditions were not discussed because of the limitation of ENVI-met, as already discussed in section 1.3.2 that wind speed and its direction remains fixed throughout the simulation period. Therefore, the wind speed was intentionally kept low at 0.5m/s in order to maintain its effect at a modest level, so that the effect of geometry on air temperature and mean radiant temperature is the focus of the case-study comparison. In practice, during field measurements, the wind speed of the traditional area (average wind speed 3.2 m/s) was found to be significantly higher than the formal area (average wind speed 0.1 m/s) which will have influenced the comfort situation in the former. Despite the higher wind speeds in the traditional area, these areas were still assumed to achieve cooler conditions than the formal areas due to the higher aspect ratio. In order to examine this, wind effect was intentionally minimised in the simulation model. Urban geometry parameters were same as Step 2 as presented in Table 3. Input data of the case-study models are presented in Table 5.

Step 3 has used simple forcing without the hourly input options for air temperature and relative humidity, in order to let the model determine those on the basis of the geometry.

Table 5. Input data for case-study models in Step 3

| | TRA1EW | TRA1NS | FRA2EW | FRA2NS |
|---|---|------------------|------------------|-------------------------|
| Canyon orientation | east-west (EW) | north-south (NS) | east-west (EW) | north-south (NS) |
| Model area | | | | |
| Main Model Area | 76m x 58m | 60m x 156m | 76m x 58m | 60m x 156m |
| Grid Size in metre | dx=2, | dx=2, | dx=2, | dx=2, |
| Dx = size of X grid | dy=2, | dy=2, | dy=2, | dy=2, |
| Dy = size of Y grid | dz=3 | dz=3 | dz=3 | dz=3 |
| Dz = size of Z grid | | | | |
| Construction material | | | | |
| Building Material | Wall: 10" brick wall (burned), Roof: light-weight concrete | same | same | same |
| Soil | Road: asphalt, Pavement: paved concrete-grey | same | same | same |
| Position | | | | |
| Longitude (°) | 90.23 | same | same | same |
| Latitude (°) | 23.24 | same | same | same |
| Start and duration of the model | | | | |
| Date of simulation | 05/04/2015 | same | same | same |
| Start time | 04:00 | same | same | same |
| Total simulation time (h) | 20 | same | same | same |
| Initial meteorological conditions | | | | |
| Roughness length at measurement site | 0.1 | same | same | same |
| Initial temperature of atmosphere (k) | 32.35°C | same | same | same |
| Simple forcing: Air temperature (%) | Min 300, at 05:00 h; Max 311, at 14:00 h | same | same | same |
| Simple forcing: Relative humidity (%) | Min 43, at 14:00 h; Max 87, at 05:00 h | same | same | same |
| Specific humidity at model top (2500 mg/kg) | 7 | same | same | same |
| Wind speed measured at 10m height (m/s) | 0.5 | same | same | same |
| Wind direction (deg) (0° = from North, 180° = from South) | 135 | 135 | 135 | 135 |
| Cover of low clouds (octas) | 0 | 0 | 0 | 0 |
| Cover of medium clouds (octas) | 0 | 0 | 0 | 0 |
| Cover of high clouds (octas) | 0 | 0 | 0 | 0 |
| Soil data, for all models | | | | |
| | Soil layer (name) | Soil layer (cm) | Soil Wetness (%) | Initial temperature (K) |
| | Upper layer | 0 – 20 cm | 50 | 293 |
| | Middle layer | 20 – 50 cm | 60 | 293 |
| | Deep layer | 50 – 200 cm | 60 | 293 |
| | Bedrock layer | Below 200 cm | 60 | 293 |

1.5. Results and discussion

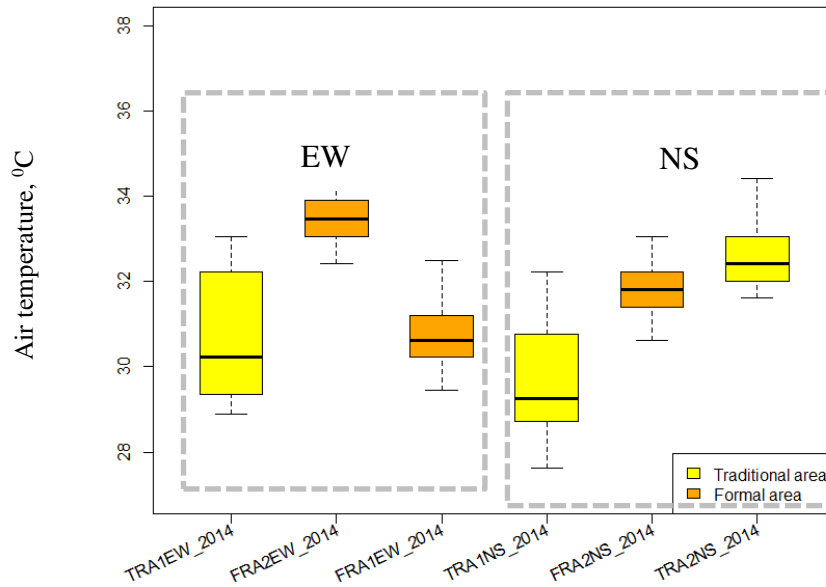
1.5.1. Analysis of results of Step 1

Table 6. Average air temperature during survey days between 12:00-15:00

| Microclimate site name (abbreviated) | Average Air temperature: Weather Station Data during 12:00-15:00 | |
|--------------------------------------|--|-------------|
| | Autumn 2014 | Summer 2015 |
| TRA1EW | 31.5 | 33.7 |
| TRA1NS | 31.5 | X |
| TRA2NS | 33.5 | 31.3 |
| FRA1EW | 29 | 31.0 |
| FRA2EW | 31.5 | 34.5 |
| FRA2NS | 31.5 | 34.5 |

Box plot analysis and related statistics of autumn 2014 and summer 2015 data are presented in Figure 4 and Figure 5 respectively. In Figure 4, both EW and NS oriented streets of the formal area FRA2 have a higher air temperature compared to the traditional area TRA1. The average (median) air temperatures of the formal sites FRA2EW and FRA2NS are 3.3⁰C and 2.5⁰C higher than the corresponding traditional sites TRA1EW and TRA1NS respectively. Among the EW oriented canyons, the site FRA1EW has the lowest maximum air temperature, due to the fact that the survey was conducted on a comparatively cooler day (see Table 6). On the contrary, TRA2NS has the highest maximum air temperature among all sites as the site was surveyed on the hottest day among the survey days during autumn 2014 (Table 6). However, the variation in average synoptic air temperature in the sites FRA1EW and TRA2NS do not affect the other four sites in FRA2 and TRA1, as these sites had equal average synoptic air temperatures (Table 6).

Similar to autumn 2014, both traditional sites TRA1EW and TRA2NS are found to have lower air temperatures compared to the corresponding formal sites in summer 2015 (Figure 5). On average (median), TRA1EW was 1.7⁰C and 2.4⁰C cooler than FRA2EW and FRA1EW respectively, while TRA2NS was 0.8⁰C cooler than FRA2NS. Although the average synoptic air temperature for FRA2EW was already 0.8⁰C warmer (Table 6) than that of TRA1EW, the formal site was still found to be 0.9⁰C warmer than the traditional site when the synoptic effect is deducted.

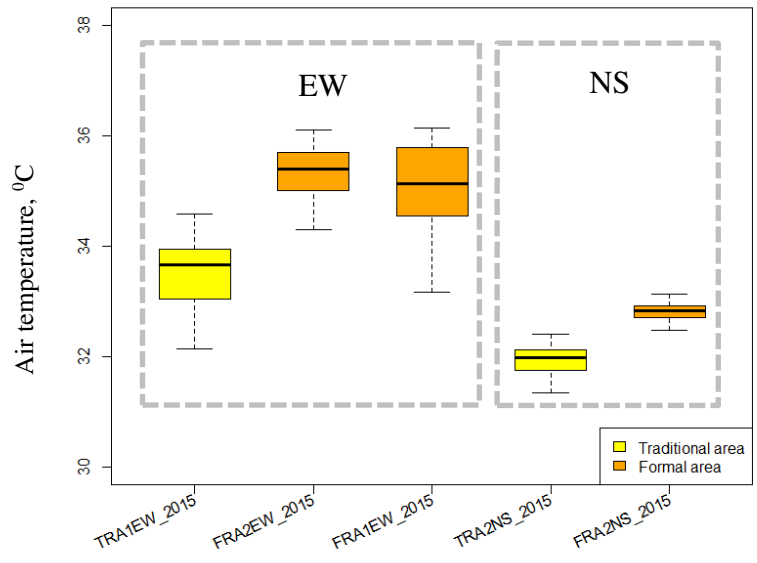


| Box plot statistics | | | | | | |
|---------------------|-------------|-------------|-------------|-------------|-------------|-------------|
| Site name | TRA1EW_2014 | FRA2EW_2014 | FRA1EW_2014 | TRA1NS_2014 | FRA2NS_2014 | TRA2NS_2014 |
| Minimum | 28.9 | 32.4 | 29.5 | 27.6 | 30.6 | 31.6 |
| Lower quartile | 29.4 | 33.1 | 30.2 | 28.7 | 31.4 | 32.0 |
| Median | 30.2 | 33.5 | 30.6 | 29.3 | 31.8 | 32.4 |
| Upper quartile | 32.2 | 33.9 | 31.2 | 30.8 | 32.2 | 33.1 |
| Maximum | 33.1 | 34.3 | 32.5 | 32.2 | 33.1 | 34.4 |

Figure 4. Comparison of air temperature across all residential sites between 12:00-15:00 during autumn 2014

Also, from a 5-minute interval data (autumn 2014), the highest difference in air temperature between FRA2EW and TRA1EW is 6.2⁰C occurring at 11:40 (Figure 6a). For north-south canyons, the highest difference is 5.0⁰C occurring at 11:55. For summer 2015 data, the corresponding differences are 3.7⁰C and 1.8⁰C between FRA2EW and TRA1EW and between FRA2Ns and TRA2NS respectively (Figure 6b). North-south canyons in both traditional and formal areas have constantly lower air temperatures in comparison to east-west canyons as can be seen in both Figure 4 and Figure 6.

In terms of mean radiant temperature, the box plots show that traditional sites in both east-west and north-south orientations have lower Tmrt values than the corresponding canyons in formal areas (Figure 7 and Figure 8). The only exceptions are FRA1EW and TRA2NS, having the coolest and warmest synoptic conditions respectively, as mentioned above. For EW canyons, the average difference (median) between FRA2EW and TRA1EW is 1.8⁰C and for NS canyon the difference between FRA2NS and TRA1NS is 2.3⁰C during autumn 2014.



| Box plot statistics | | | | | |
|---------------------|-------------|-------------|-------------|-------------|-------------|
| Site name | TRA1EW_2015 | FRA2EW_2015 | FRA1EW_2015 | TRA2NS_2015 | FRA2NS_2015 |
| Minimum | 32.1 | 34.3 | 33.2 | 31.3 | 32.5 |
| Lower quartile | 33.0 | 35.0 | 34.6 | 31.7 | 32.7 |
| Median | 33.7 | 35.4 | 35.1 | 32.0 | 32.8 |
| Upper quartile | 33.9 | 35.7 | 35.8 | 32.1 | 32.9 |
| Maximum | 34.6 | 36.1 | 36.1 | 32.4 | 33.1 |

Figure 5. Comparison of air temperature across all residential sites between 12:00-15:00 during summer 2015

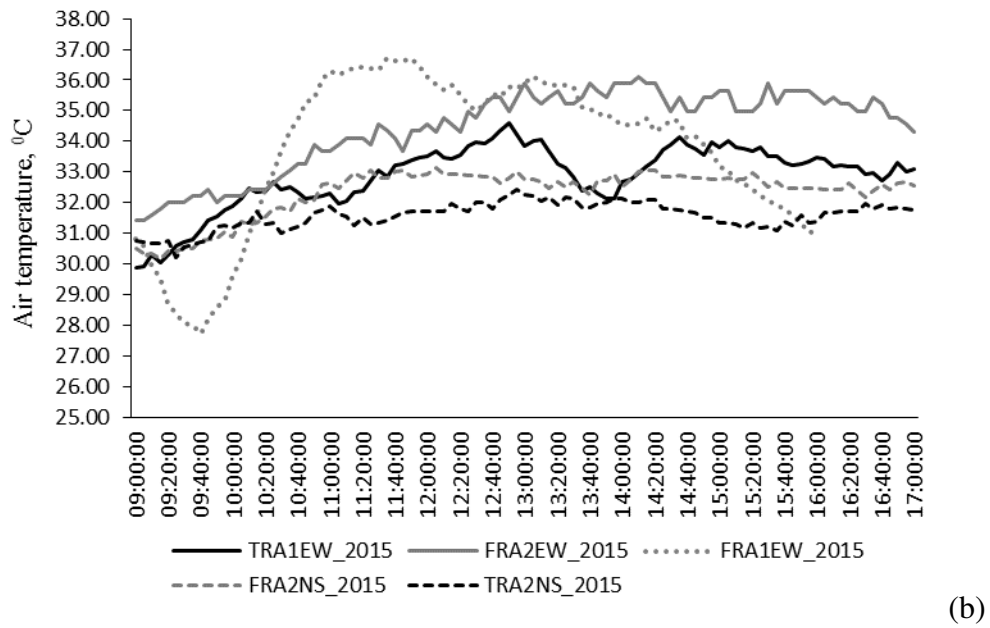
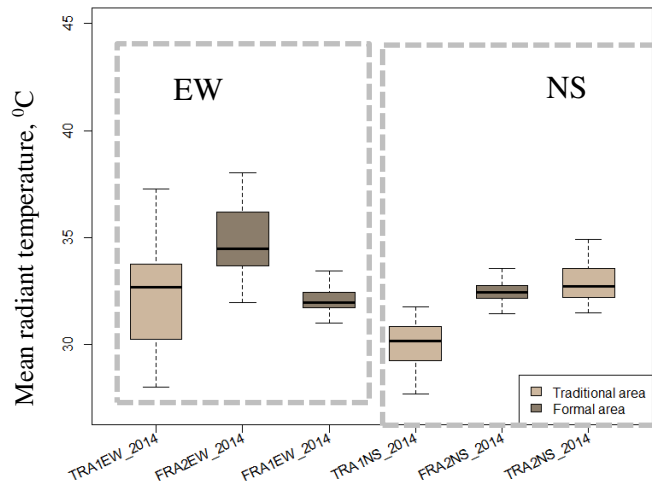
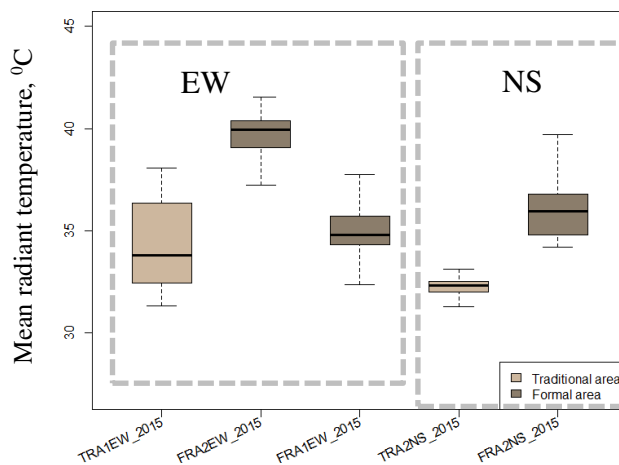


Figure 6 Progression of air temperature during 09:00-17:00 in Step 1: a) autumn 2014, b) summer 2015



| Box plot statistics | | | | | | |
|---------------------|-------------|-------------|-------------|-------------|-------------|-------------|
| Site name | TRA1EW_2014 | FRA2EW_2014 | FRA1EW_2014 | TRA1NS_2014 | FRA2NS_2014 | TRA2NS_2014 |
| Minimum | 28.0 | 32.0 | 31.0 | 27.7 | 31.5 | 31.5 |
| Lower quartile | 30.3 | 33.7 | 31.7 | 29.2 | 32.2 | 32.2 |
| Median | 32.7 | 34.5 | 32.0 | 30.2 | 32.5 | 32.7 |
| Upper quartile | 33.8 | 36.2 | 32.4 | 30.9 | 32.8 | 33.6 |
| Maximum | 37.3 | 38.1 | 33.5 | 31.8 | 33.6 | 34.9 |

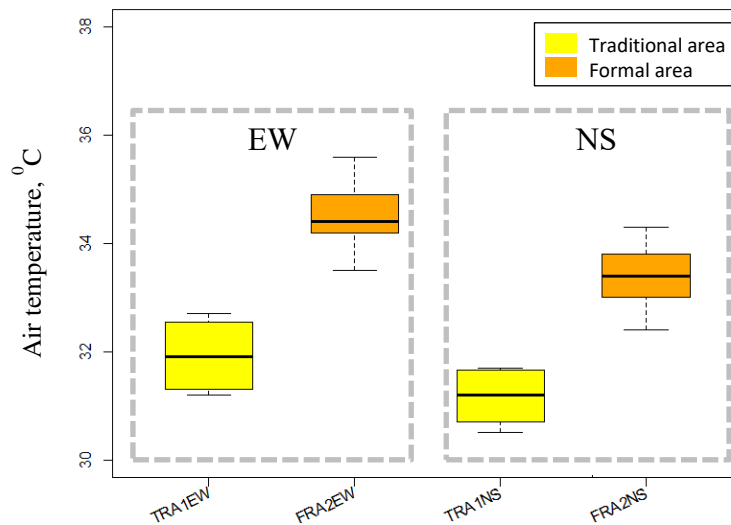
Figure 7. Comparison of mean radiant temperature across all residential sites between 12:00-15:00 during autumn 2014



| Box plot statistics | | | | | |
|---------------------|-------------|-------------|-------------|-------------|-------------|
| Site name | TRA1EW_2015 | FRA2EW_2015 | FRA1EW_2015 | TRA2NS_2015 | FRA2NS_2015 |
| Minimum | 31.3 | 37.2 | 32.4 | 31.3 | 34.2 |
| Lower quartile | 32.4 | 39.1 | 34.3 | 32.0 | 34.8 |
| Median | 33.8 | 40.0 | 34.8 | 32.3 | 36.0 |
| Upper quartile | 36.4 | 40.4 | 35.7 | 32.5 | 36.8 |
| Maximum | 38.1 | 41.5 | 37.7 | 33.1 | 39.7 |

Figure 8. Comparison of mean radiant temperature across all residential sites between 12:00-15:00 during summer 2015

1.5.2. Analysis of results of Step 2



| Box plot statistics | | | | |
|---------------------|--------|--------|--------|--------|
| Site name | TRA1EW | FRA2EW | TRA1NS | FRA2NS |
| Minimum | 31.2 | 33.5 | 30.5 | 32.4 |
| Lower quartile | 31.3 | 34.2 | 30.7 | 33.0 |
| Median | 31.9 | 34.4 | 31.2 | 33.4 |
| Upper quartile | 32.6 | 34.9 | 31.7 | 33.8 |
| Maximum | 32.7 | 35.6 | 31.7 | 34.3 |

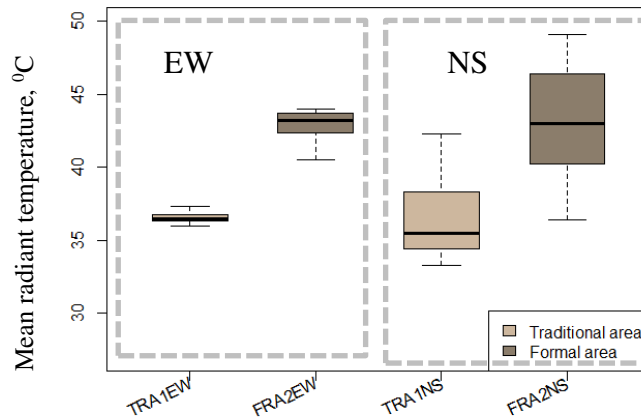
Figure 9. Comparison of air temperature in simulated case-study areas between 12:00-15:00 in Step 2

In Step 2, a comparison is done between ENVI-met simulated models of the traditional and formal case-study areas. As mentioned in section 3.4.5, site-specific measured data is used as boundary condition for simulated models in ENVI-met. The main idea is to examine whether any microclimatic difference is occurring between the traditional and formal areas for the simulated models as observed during the field measurements.

Resembling the field measurements in Step 1, both east-west (EW) and north-south (NS) canyons in traditional areas in Step 2 are found to have lower air temperature values than their corresponding canyons in formal areas (Figure 9). The average (median) values of FRA2EW and FRA2NS are higher from the average (median) values of TRA1EW and TRA1NS by 2.5⁰C and 2.2⁰C respectively (Figure 9).

Similar to field measurements, average (median) T_{mrt} in both EW and NS canyons in the traditional area are also found to be lower than those in the formal area (Figure 10). The differences are 6.7⁰C and 7.5⁰C for EW and NS canyons respectively. This is larger than the

differences reported in field measurements in autumn 2014 (1.8⁰C and 2.3⁰C respectively). Among all four canyons TRA1EW has the smallest and lowest Tmrt range between 36.3-37.8⁰C with 50% of the data, making it the coolest site. On the other hand, FRA2NS has the largest range between first and third quartile of 40.3 - 46.4⁰C, thus making it the hottest site. The maximum Tmrt for all canyons lies between 37.3 - 49.1⁰C, whereas the maximum values for field measurements lie between 31.8 - 38.1⁰C. This shows Tmrt is overestimated in the simulation models.

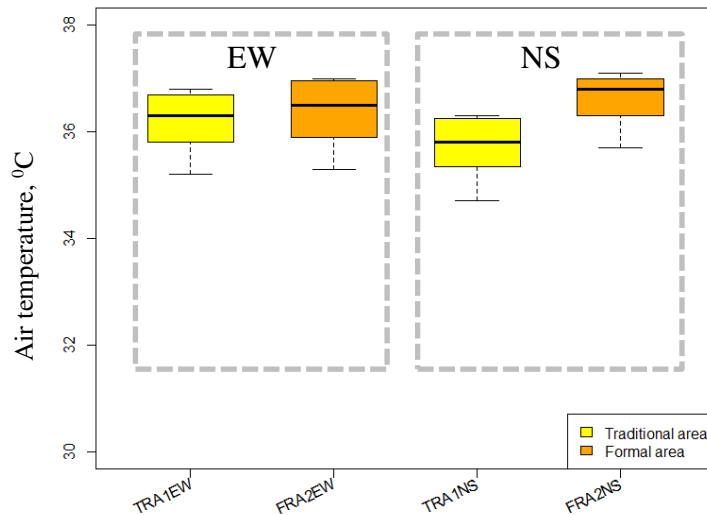


| Box plot statistics | | | | |
|---------------------|--------|--------|--------|--------|
| Site name | TRA1EW | FRA2EW | TRA1NS | FRA2NS |
| Minimum | 36.0 | 40.5 | 33.3 | 36.4 |
| Lower quartile | 36.3 | 42.4 | 34.4 | 40.3 |
| Median | 36.5 | 43.2 | 35.5 | 43.0 |
| Upper quartile | 36.8 | 43.7 | 38.3 | 46.4 |
| Maximum | 37.3 | 44.0 | 42.3 | 49.1 |

Figure 10. Comparison of mean radiant temperature in simulated case-study areas between 12:00-15:00 in Step 2

1.5.3. Analysis of results of Step 3

Similar to Step 2, Step 3 also presents a comparison between ENVI-met simulated models of the traditional and formal case-study areas. The difference between Step 2 and Step 3 is, instead of site-specific measured data, a worst-case boundary condition has been used in Step 3 and this has been kept identical across all simulation models.



| Box plot statistics | | | | |
|---------------------|--------|--------|--------|--------|
| Site name | TRA1EW | FRA2EW | TRA1NS | FRA2NS |
| Minimum | 35.2 | 35.3 | 34.7 | 35.7 |
| Lower quartile | 35.8 | 35.9 | 35.4 | 36.3 |
| Median | 36.3 | 36.5 | 35.8 | 36.8 |
| Upper quartile | 36.7 | 37.0 | 36.3 | 37.0 |
| Maximum | 36.8 | 37.0 | 36.3 | 37.1 |

Figure 11. Comparison of air temperature in simulated case-study areas between 12:00-15:00 in Step 3

The result shows, there is negligible difference in air temperature between the case-study areas simulated using the same climatic information (Figure 11). The average (median) air temperature for all sites has a standard deviation of only 0.4. The difference is especially insignificant between FRA2EW and TRA1EW, with only 0.2⁰C difference in median values in comparison to the 3.3⁰C difference reported in field studies (Figure 4). However, a slightly higher difference of around 1.0⁰C (median) is found between FRA2NS and TRA1NS, but this is still below the average difference of 2.5⁰C between the sites reported in the field studies (Figure 4).

Even though small differences are visible in terms of air temperature between the case-study areas simulated using same climatic information, Tmrt shows large variations in terms of median and interquartile ranges (Figure 12). While the sites FRA2EW, TRA1NS and FRA2NS have a larger interquartile range for Tmrt that lies between 55.4 – 70.9⁰C, TRA1EW has a narrower interquartile range that lies between 58.9 – 61.3⁰C (Figure 12). During the field-study (Step 1), TRA1NS was reported to be the coolest site with the smallest interquartile range

between 29.2-30.9⁰C (Figure 7). Differences in median values between TRA1EW and FRA2EW is 8.7⁰C (against 1.8⁰C in field-study) and between TRA1NS and FRA2NS is 10.9⁰C (against 2.3⁰C in field-study).

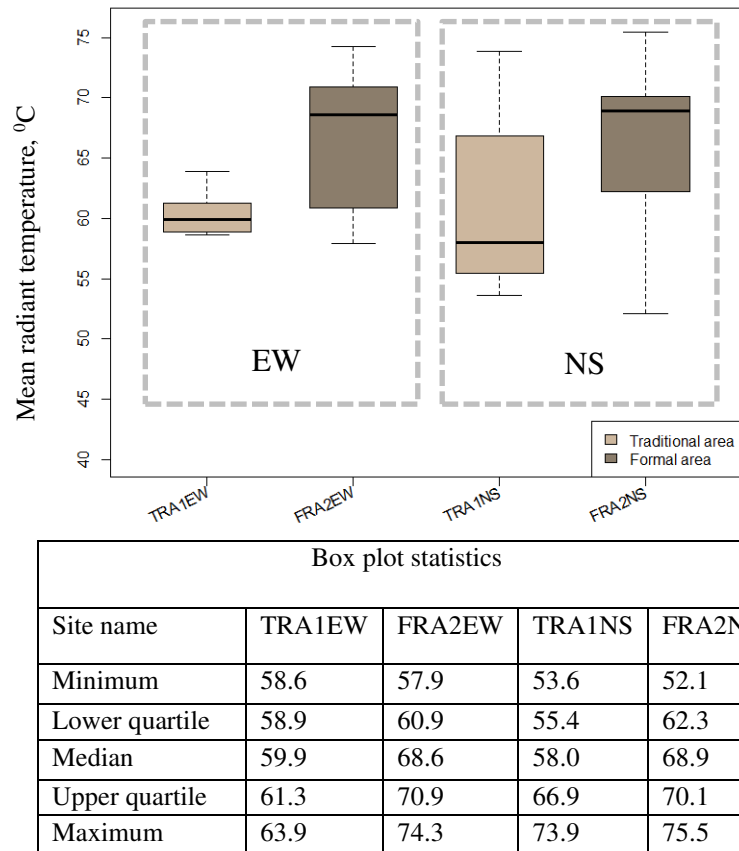


Figure 12. Comparison of mean radiant temperature in simulated case-study areas between 12:00-15:00 in Step 3

1.5.4. Comparison between the steps

While the above sections (1.5.1, 1.5.2 and 1.5.3) have presented a comparison between the traditional and formal areas in each step, this section (1.5.4) presents a comparison between the steps.

1.5.4.1. Air-temperature

Since the models in Step 2 and Step 3 have different boundary conditions, it is not possible to compare the case-study areas directly to each other. It was thought more appropriate to compare the differences among the traditional and formal sites in one step with the differences between them in the other step.

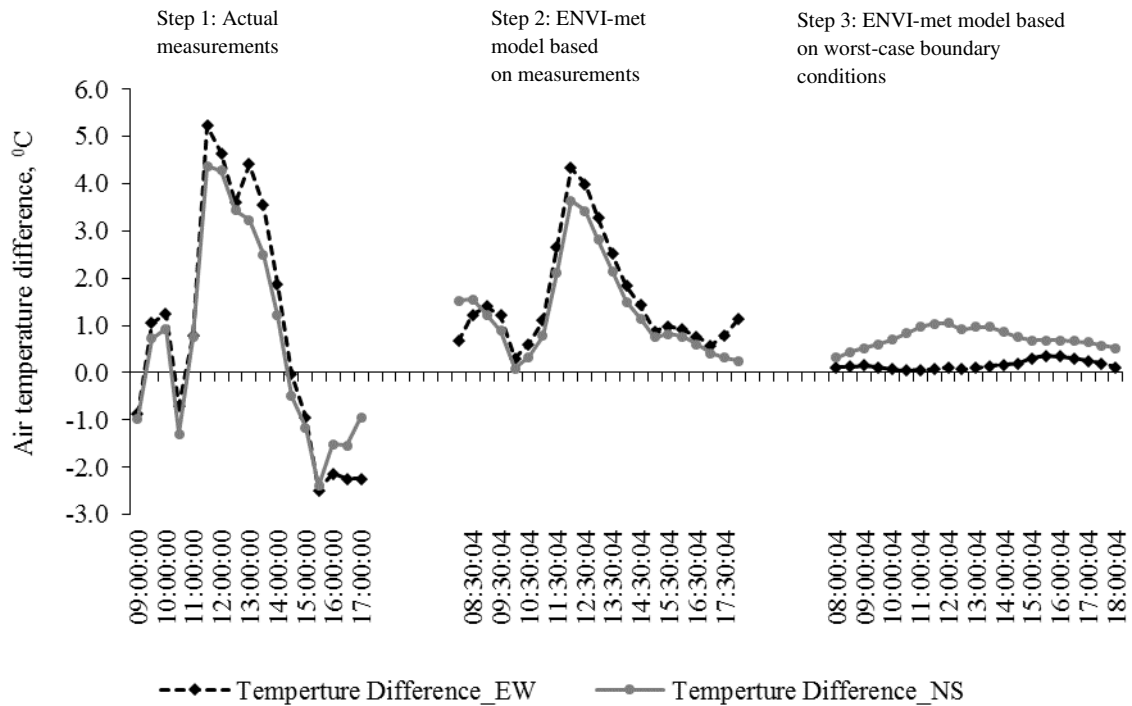


Figure 13. Air temperature difference between traditional and formal residential areas in east-west and north-south canyons in Step 1, Step 2 and Step 3

Table 7. Correlation between climatic variables in Step 1 and Step 2

| Site Name | Ta | Tmrt | ν | RH |
|-----------|--------------------------|-----------------------------------|--------------------------|--------------------------|
| | Pearson's r (p value) | Pearson's r (p value) | Pearson's r (p value) | Pearson's r (p value) |
| TRA1EW | 0.79 (0.000) | 0.60 (0.01) | -0.75 (0.000) | 0.72 (0.000) |
| TRA1NS | 0.80 (0.000) | 0.32 (0.7) ¹¹ | -0.56 (0.01) | 0.71 (0.000) |
| FRA2EW | 0.90 (0.000) | 0.76 (0.000) | 0.42 (0.07) | 0.92 (0.000) |
| FRA1NS | 0.87(0.000) | 0.68 (0.001) | 0.69 (0.002) | 0.75 (0.000) |

Significant differences were found in air temperature between the formal and traditional areas in both EW and NS canyons during field measurements (Figure 6a,b). Half-hourly variations show up to 5.2⁰C and 4.4⁰C differences in EW and NS canyons respectively between formal and traditional areas (Figure 13). The maximum differences, based on a 5-minute frequency, were found to be 6.2⁰C and 5.0⁰C (Figure 6a). The side-by-side comparison of the scenarios is presented in Figure 13 to assist the comparison of field measurements (Step 1) with the simulated Steps (Step 2, Step 3). Other research has reported a 7.0⁰C air temperature variation from field-study measurements between sites with various aspect ratios in a similar climate in Colombo (Emmanuel & Johansson 2006). Furthermore, a previous study in the

¹¹ p value represents non-significant correlation.

related context in Dhaka has also found 4.5⁰C variation in maximum air temperature in urban canyons with an aspect ratio between 0.3 and 2.8 (Ahmed, 1994).

Table 8. Correlation between climatic variables in Step 1 and Step 3

| Difference | Site Name | Ta | Tmrt | ν | RH |
|--|-----------------|--------------------------|--------------------------|--------------------------|--------------------------|
| | | Pearson's r (p value) | Pearson's r (p value) | Pearson's r (p value) | Pearson's r (p value) |
| Difference in EW canyons between formal and traditional area | TRA1EW & FRA2EW | -0.57 (0.32) | -0.25 (0.39) | 0.39 (0.16) | -0.62 (0.02) |
| Difference in NS canyons between formal and traditional area | TRA1NS & FRA1NS | 0.77 (0.001) | 0.24 (0.39) | 0.53 (0.05) | 0.61(0.02) |

When the case-study areas were simulated using the climatic information from the field-study (Step 2), air temperature shows high proximity to the actual values (Step 1). A correlation analysis between the measured and simulated values (Table 7) shows correlation and significance (p-values) for air temperature. In this case (Step 2), the differences between the traditional and formal areas were similar to the differences found in the field-study (Figure 13). However, in Step 3, the correlation analysis in Table 8 shows that the difference in EW canyons between the formal and traditional area reported during field-measurements is inversely correlated with the differences between them in simulation models. Even though the differences in the NS canyon is positively correlated, the differences reported in the simulation model is much lower than the actual differences reported during the field-measurements (Figure 13).

The sites were chosen because of their similarities with respect to key determinants of the urban microclimate (materials, albedo, vegetation, etc.) with only urban form being different. In simulation models (Step 2 and Step 3), the same building material and albedo are assumed for all cases. Therefore, the resultant microclimatic conditions are primarily a function of the geometry of the sites. The results from Figure 13 and Table 8 indicate that ENVI-met is unable to distinguish between geometric variations in terms of air temperature.

The H/W ratios of the case-study areas TRA1EW and FRA2EW are 3.2 and 1.8 respectively (Table 3). The height variability, measured by the standard deviation of H/W ratio (H/W ratio_STDEV), of the sites TRA1EW and FRA2EW are 0.34 and 0.05 and of the sites

TRA1NS and FRA2NS are 0.85 and 0.0 respectively (Table 3). While the standard deviation of H/W ratio represents physical diversity in the traditional areas, the standard deviation of SVF (SVF_STDEV) did not properly represent their variability as the canyons are already very compact and narrow. Krüger et al. (2011) in their investigation of urban geometry in Curitiba, Brazil also found that in spite of irregularities in building heights and location on a crossing street, some measurement points had similar SVF values. The study further suggests that SVF is not an effective parameter to explain irregularities in dense urban geometries. However, in spite of the difference between the sites in H/W ratio and H/W ratio_STDEV, there was almost no deviation in air temperature in the simulated models in Step 3. This suggests ENVI-met is not sensitive enough to the irregularity of urban geometry characteristics as can be seen in real conditions. Other studies have also reported inaccurate evaluations of surface albedo and air temperature (Acero & Herranz-Pascual 2015).

Air temperature in ENVI-met is calculated by the combined advection-diffusion equation in which the change in air temperature is affected by the deviation of the long wave radiation (Huttner 2012). The limitations in measuring the long wave radiation in ENVI-met could have affected the calculation of air temperature in Step 3. When hourly forcing of air temperature is used in the modelling, a correlation up to 0.97 ($r = 0.90$ in this study, Table 7) has been found between the measured and modelled values (Acero & Herranz-Pascual 2015). However, when using only simple forcing (not hourly forcing), the differences between geometric characters (standard deviation of H/W ratio in particular) of the case-study areas remain unexplained in modelling and are unable to produce expected differences.

The authors of ENVI-met V4 (Bruse 2016) suggests that ENVI-met has a tendency to underestimate the dynamics of the diurnal temperature amplitude (<http://www.envi-met.com/documents/onlinehelpv3/hs880.htm>). There are two reasons for this:

- When ENVI-met simulation is carried out in a non-forced (or non-nested) way, it can often underestimate the dynamic of air temperature as the larger regional effects are not taken into account,
- Heating and cooling of air layers due to a divergence of vertical long wave radiation are not included in the air temperature equations.

Estimating the effect of the second aspect alone is particularly complex because of several counter-acting mechanisms. It is especially difficult because long wave fluxes inside urban environments are very complex and not only driven by vertical fluxes but also by

horizontal fluxes. Therefore, it was too complex to be included in the earlier model versions. However, there has been some improvement in ENVI-met V4 in recognising the long wave flux divergence. But as the results of this study indicate, it is still essential to use site specific boundary information to produce authentic results in ENVI-met.

1.5.4.2. Mean radiant temperature

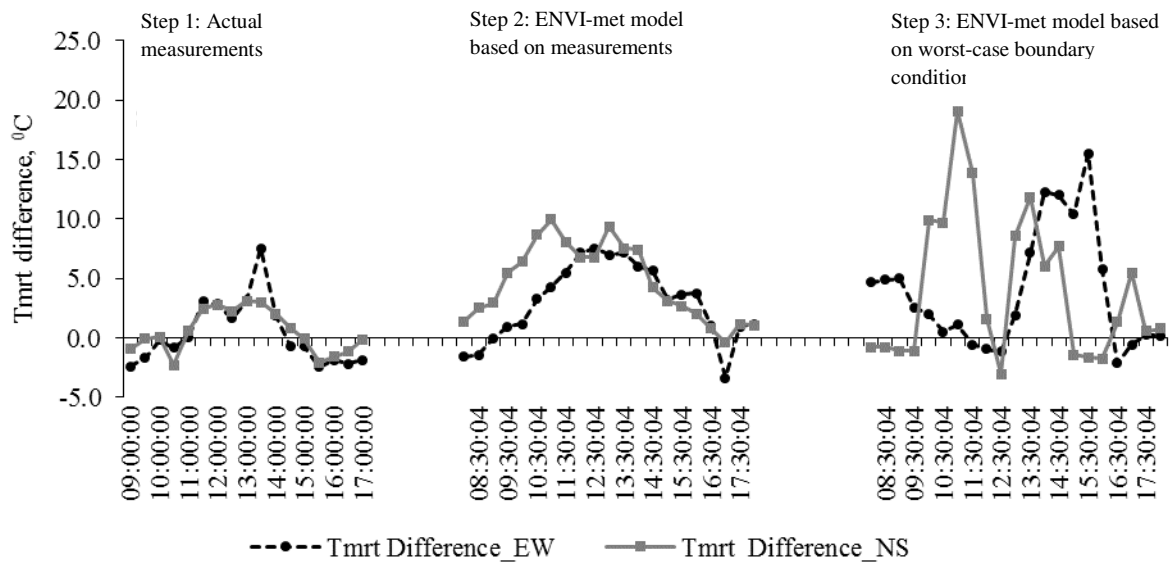


Figure 14. Tmrt difference between traditional and formal residential areas in east-west and north-south canyons in Step 1, Step 2 and Step 3

As can be seen in Figure 14, both simulation models (Step 2 and Step 3) have predicted that Tmrt measures in the formal area are higher than the same in the traditional area similar to the field measurements (Step 1). Although they are overestimated in both cases, Tmrt measures in Step 3 are unrealistically high. This is very different from real situations because model boundary conditions are not similar to actual conditions. A worst-case scenario with a cloudless condition is assumed for Step 3 and for this reason Tmrt conditions are significantly higher than the actual situation. Subsequently, instead of actual values of Tmrt, the correlation between the measured and simulated (Step 3) differences between traditional and formal areas has been examined in Table 8. The results reveal negative (positive for NS canyon) and weak correlations with statistically non-significant p values for EW and NS canyons.

In this study, Tmrt in the ENVI-met simulations is further overestimated due to the fact that ENVI-met has a tendency to calculate higher shortwave radiation during the daytime (Acero & Herranz-Pascual 2015). Along with shortwave radiation, errors have been reported in calculating diffused and reflected shortwave radiation and long wave radiation. An overall

imprecise calculation of the radiation fluxes is reported by Huttner (2012). Furthermore, the shadow pattern can vary substantially due to the horizontal model resolution which leads to a significant T_{mrt} variation in the clear sky conditions. The exposure to direct solar radiation can also be miscalculated by approximate estimation of building heights as well as the resolution of the vertical grid. However, this study is more interested in relative differences between the case-study sites, rather than comparing the absolute values of simulation results with the actual measurements.

1.6. Conclusion

Recent studies have shown that the geometry and the aspect ratio of urban canyons play a crucial role in moderating the microclimate at the street level (Shashua-Bar et al. 2004). This study has examined the shortcomings of modelling techniques in responding sufficiently to the urban geometry characteristics, such as H/W ratio and its standard deviation, SVF and its standard deviation. It has addressed a specific argument: whether microclimatic modelling techniques can address the impact of diversity of urban form, as addressed by the H/W ratio and its standard deviation; to find out what the limitations are; and what could be done to improve their implementation in assessing microclimatic conditions. To find the answer, actual case-study areas were simulated using the same boundary conditions to investigate the impact of physical diversity upon resultant environmental characteristics.

The case study areas in this study represent formal and traditional residential areas in Dhaka with distinct urban geometry features; the formal area having mostly uniform character and the traditional area having a diverse geometric character. Direct microclimatic monitoring results in Step 1 shows a 3.3°C average (median) and 6.2°C maximum air temperature difference between the formal and traditional areas. In terms of T_{mrt} , the average (median) and maximum differences were 2.3°C and 10.0°C respectively. In Step 2, ENVI-met simulation models of the case study areas (modelled using the actual field study data as the boundary condition) shows, the difference found between the simulation models of the traditional and formal areas in terms of air temperature is similar to the difference found between the actual sites from field measurements. In Step 3, case study areas are modelled using identical boundary conditions across all models to see how the urban geometry variation between the sites affect air temperature and other microclimatic variables. Air temperature differences among the simulation models of the formal and traditional areas were found small or insignificant, 0.2°C for EW canyon and 1.0°C for NS canyon. A significant discrepancy was

seen in mean radiant temperature as well. Tmrt values were overestimated. This shows that unless the site-specific climatic information is used as an input, ENVI-met is unable to produce microclimatic conditions resulting from the physical variation of the areas.

The results from this study imply that it is necessary to use the most characteristic weather information from a case-study areas in lieu of synoptic weather information as boundary conditions to produce credible results in ENVI-met. The results produced in this manner could reveal differences in urban geometry and capture their consequences on microclimatic conditions. Thus, even though ENVI-met is a useful tool for examining typical meteorological conditions, users need to be aware of the above limitations while using the modelling techniques. Simple and regular urban arrays can be assessed effectively in terms of their relative performances, but the complexity of urban forms of real cities provides important environmental advantages and richness that should not be overlooked.

Acknowledgements

This paper is drawn from research funded by the Schlumberger Foundation at the University of Cambridge, Department of Architecture.

References

- Acero, J. a. & Herranz-Pascual, K., 2015. A comparison of thermal comfort conditions in four urban spaces by means of measurements and modelling techniques. *Building and Environment*, 93, pp.245–257. doi:10.1016/j.buildenv.2015.06.028.
- Ahmed, K.S., 1994. A comparative analysis of the outdoor thermal environment of the urban vernacular and the contemporary development: case studies in Dhaka. In *Architecture of the Extremes: 11th PLEA International Conference*. pp. 3–8.
- Ahmed, K.S., 1994. Comparative analysis of the outdoor thermal environment of the urban vernacular and the contemporary development: case studies in Dhaka. In *Architecture of the Extremes*.
- Ali-Toudert, F. & Mayer, H., 2007. Effects of asymmetry, galleries, overhanging facades and vegetation on thermal comfort in urban street canyons. *Solar Energy*, 81(6), pp.742–754. doi:10.1016/j.solener.2006.10.007.
- Arnfield, A.J., 2003. Two decades of urban climate research: A review of turbulence, exchanges of energy and water, and the urban heat island. *International Journal of Climatology*, 23(1), pp.1–26. doi:10.1002/joc.859.
- Barlow, J.F., 2014. Progress in observing and modelling the urban boundary layer. *Urban Climate*, 10(P2), pp.216–240. doi:10.1016/j.uclim.2014.03.011.
- Bourbia, F. & Awbi, H.B., 2004. Building cluster and shading in urban canyon for hot dry climate Part 1: Air and surface temperature measurements. *Renewable Energy*, 29(2), pp.249–262. doi:10.1016/S0960-1481(03)00170-8.
- Bourbia, F. & Boucheriba, F., 2010. Impact of street design on urban microclimate for semi

- arid climate (Constantine). *Renewable Energy*, 35(2), pp.343–347. doi:10.1016/j.renene.2009.07.017.
- Bruse, M., 2015. ENVI-met 4: A Microscale Urban Climate Model.
- Bruse, M., 2016. ENVI-met Knowledge Base: Longwave Flux Divergence.
- Bruse, M., 1999. Modelling and strategies for improved urban climates. *Biometeorology and urban climatology at the turn of the millenium, Sydney, 8-12 novembre 1999*, p.6p.
- Bruse, M. & Fleer, H., 1998. With a Three Dimensional Numerical Model. *Environmental Modelling & Software*, 13(3–4), pp.373–384.
- Chen, L. et al., 2012. Sky view factor analysis of street canyons and its implications for daytime intra-urban air temperature differentials in high-rise, high-density urban areas of Hong Kong: A GIS-based simulation approach. *International Journal of Climatology*, 32(1), pp.121–136. doi:10.1002/joc.2243.
- Colaninno, N., Cladera, J. & Pfeffer, K., 2011. An automatic classification of urban texture: form and compactness of morphological homogeneous structures in Barcelona. In *New Challenges for European Regions and Urban Areas in a Globalised World*. Barcelona, Spain.
- de Dear, R., 1987. Ping-pong globe thermometers for mean radiant temperatures. *Heating and Ventilating Engineer and Journal of Air Conditioning*, 60(681), pp.10–11.
- Earth, G., 2015. Dhaka, Bangladesh.23046°02.75” N and 90025°10.32” E.
- Emmanuel, R. & Johansson, E., 2006. Influence of urban morphology and sea breeze on hot humid microclimate: the case of Colombo, Sri Lanka. *Climate Research*, 30(3), pp.189–200. doi:10.3354/cr030189.
- Erell, E., Pearlmutter, D. & Williamson, T., 2012. *Urban Microclimate: Designing the Spaces Between Buildings*, Routledge.
- Huttner, S., 2012. Further development and application of the 3D microclimate simulation ENVI-met.
- ISO 7726, 1998. *Ergonomics of the Thermal Environment – Instruments for Measuring Physical Quantities*, Geneva.
- Johansson, E., 2006. Influence of urban geometry on outdoor thermal comfort in a hot dry climate: A study in Fez, Morocco. *Building and Environment*, 41(10), pp.1326–1338. doi:10.1016/j.buildenv.2005.05.022.
- Kikegawa, Y. et al., 2006. Impacts of city-block-scale countermeasures against urban heat-island phenomena upon a building’s energy-consumption for air-conditioning. *Applied Energy*, 83(6), pp.649–668. doi:10.1016/j.apenergy.2005.06.001.
- Krüger, E.L., Minella, F.O. & Rasia, F., 2011a. Impact of urban geometry on outdoor thermal comfort and air quality from field measurements in Curitiba, Brazil. *Building and Environment*, 46(3), pp.621–634. doi:10.1016/j.buildenv.2010.09.006.
- Krüger, E.L., Minella, F.O. & Rasia, F., 2011b. Impact of urban geometry on outdoor thermal comfort and air quality from field measurements in Curitiba, Brazil. *Building and Environment*, 46(3), pp.621–634. doi:10.1016/j.buildenv.2010.09.006.
- Lindberg, F., Holmer, B. & Thorsson, S., 2008. SOLWEIG 1.0 – Modelling spatial variations of 3D radiant fluxes and mean radiant temperature in complex urban settings. *International Journal of Biometeorology*, 52(7), pp.697–713. doi:10.1007/s00484-008-0162-7.
- Maggiotto, G. et al., 2014. Validation of temperature-perturbation and CFD-based modelling for the prediction of the thermal urban environment: The Lecce (IT) case study. *Environmental Modelling and Software*, 60, pp.69–83. doi:10.1016/j.envsoft.2014.06.001.
- Matzarakis, A., Rutz, F. & Mayer, H., 2010. Modelling radiation fluxes in simple and complex environments: Basics of the RayMan model. *International Journal of Biometeorology*,

- 54(2), pp.131–139. doi:10.1007/s00484-009-0261-0.
- Ng, E. et al., 2012. A study on the cooling effects of greening in a high-density city: An experience from Hong Kong. *Building and Environment*, 47, pp.256–271. doi:10.1016/j.buildenv.2011.07.014.
- Oke, T.R., 1987. *Boundary Layer Climates*, Psychology Press.
- Oke, T.R. et al., 1991. Simulation of surface urban heat islands under “ideal” conditions at night part 2: Diagnosis of causation. *Boundary-Layer Meteorology*, 56(4), pp.339–358. doi:10.1007/BF00119211.
- Oke, T.R., 1988. Street design and urban canopy layer climate. *Energy and Buildings*, 11(1–3), pp.103–113. doi:10.1016/0378-7788(88)90026-6.
- Qaid, A. & Ossen, D.R., 2014. Effect of asymmetrical street aspect ratios on microclimates in hot, humid regions. *International Journal of Biometeorology*, pp.657–677. doi:10.1007/s00484-014-0878-5.
- Ratti, C., 2005. The lineage of the line: Space syntax parameters from the analysis of urban DEMs. *Environment and Planning B: Planning and Design*, 32(4), pp.547–566. doi:10.1068/b31045.
- Sharmin, T., Steemers, K. & Matzarakis, A., 2015. Analysis of microclimatic diversity and outdoor thermal comfort perceptions in the tropical megacity Dhaka , Bangladesh. *Building and Environment*, 94(November), pp.734–750. doi:10.1016/j.buildenv.2015.10.007.
- Shashua-Bar, L., Tzimir, Y. & Hoffman, M.E., 2004. Thermal effects of building geometry and spacing on the urban canopy layer microclimate in a hot-humid climate in summer. *International Journal of Climatology*, 24(13), pp.1729–1742. doi:10.1002/joc.1092.
- Steeners, K. et al., 1997. City Texture and Microclimate. *Urban Design Studies*, 3, pp.25–50.
- Steeners, K. & Ramos, M., 2010. Urban environmental diversity and human comfort. In E. NG, ed. *Designing High Density Cities: For social and environmental sustainability*. London: Earthscan, pp. 107–118.
- Stewart, I.D. & Oke, T.R., 2012. Local climate zones for urban temperature studies. *Bulletin of the American Meteorological Society*, 93(12), pp.1879–1900. doi:10.1175/BAMS-D-11-00019.1.
- Tan, C.L., Wong, N.H. & Jusuf, S.K., 2014. Outdoor mean radiant temperature estimation in the tropical urban environment. *Landscape and Urban Planning*, 127, pp.52–64. doi:10.1016/j.landurbplan.2014.04.005.
- Teller, J. & Azar, S., 2001. Townscope II - A computer systems to support solar access decision-making. *Solar Energy*, 70(3), pp.187–200. doi:10.1016/S0038-092X(00)00097-9.
- Thorsson, S. et al., 2007. Different methods for estimating the mean radiant temperature in an outdoor urban setting. *International Journal of Climatology*, 1993(October), pp.1983–1993. doi:10.1002/joc.
- Xi, T. et al., 2012. Study on the outdoor thermal environment and thermal comfort around campus clusters in subtropical urban areas. *Building and Environment*, 52(July 2007), pp.162–170. doi:10.1016/j.buildenv.2011.11.006.
- Yan, H. et al., 2014. Assessing the effects of landscape design parameters on intra-urban air temperature variability: The case of Beijing, China. *Building and Environment*, 76, pp.44–53. doi:10.1016/j.buildenv.2014.03.007.
- Yang, X. et al., 2013. Evaluation of a microclimate model for predicting the thermal behavior of different ground surfaces. *Building and Environment*, 60, pp.93–104. doi:10.1016/j.buildenv.2012.11.008.